PCCP

PAPER

Check for updates

Cite this: *Phys. Chem. Chem. Phys.*, 2019, **21**, 5695

Fluorescence enhancement induced by quadratic electric-field effects on singlet exciton dynamics in poly(3-hexylthiophene) dispersed in poly(methyl methacrylate)†

Toshifumi Iimori,[a] Kamlesh Awasthi,[b] Chin-Shiun Chiou,[b] Eric Wei-Guang Diau[bc] and Nobuhiro Ohta*[bc]

Received 22nd December 2018,
Accepted 7th February 2019

DOI: 10.1039/c8cp07801g

rsc.li/pccp

The dynamics of the exciton generated by photoexcitation of a regioregular poly(3-hexylthiophene) (P3HT) polymer dispersed in a poly(methyl methacrylate) (PMMA) matrix was examined using electro-photoluminescence (E-PL) spectroscopy, where electric field effects on the photoluminescence (PL) spectra were measured. The quadratic electric-field effect was investigated using the modulation technique, with field-induced changes in the PL intensity monitored at the second harmonic of the modulation frequency of the applied electric field. Absorption and PL spectra indicated the formation of both ordered crystalline aggregates and amorphous regions of P3HT polymer chains. Although previous studies of electric field effects on π-conjugated polymers have generally shown that the PL intensity is decreased by electric fields, we report that the PL intensity of P3HT and PL lifetime increased with the quadratic electric-field effect. The magnitude of the change in PL intensity was quantitatively explained in terms of the field-induced decrease in the nonradiative decay rate constants of the exciton. We proposed that a delayed PL, originating from charge carrier recombination, was enhanced in the presence of electric fields. The rate constant of the downhill relaxation process of the exciton, which originated from the relaxation in distributed energy levels due to an inherent energetic disorder in P3HT aggregates, was implied to decrease in the presence of electric fields. The radiative decay rate constant and PL quantum yield of P3HT dissolved in solution, which were evaluated from the molar extinction coefficient and the PL lifetime, were compared with those of P3HT dispersed in a PMMA matrix.

1. Introduction

Conjugated polymers have attracted great interest among organic materials owing to their applications in inexpensive, flexible, and light-weight materials for electronic and optoelectronic devices.[1–9] Alkyl-substituted polythiophenes are known to show excellent performance as hole-transport materials, with regioregular poly-(3-hexylthiophene-2,5-diyl) (rr-P3HT) being of primary importance among alkyl-substituted polythiophenes.[10,11]

The photophysics of rr-P3HT has attracted much interest and been studied using various optical probe techniques.[12–30] Despite numerous studies, the photophysics of elementary excitation in rr-P3HT is complicated, with further studies needed to obtain a complete understanding. The complexity specific to rr-P3HT film is due to the presence of both crystalline domains, with coupling among thiophene units belonging to different polymer chains, and amorphous domains with a lower degree of polymer chain order.

The generation process and relaxation pathway of elementary excited species, such as excitons, might be influenced by the perturbation of external electric fields. Investigation of the response of excitons to external electric fields has provided us with valuable information regarding the mechanism responsible for the photophysics of π-conjugated polymers.[17,18,22,24,28,31–44] The photoluminescence (PL) quenching of both pristine films and aggregates of rr-P3HT dispersed in inert matrices induced by electric fields has been reported by different groups.[18,24,28,41,43,45] As a plausible singlet exciton quenching mechanism, dissociation of the exciton into the electron–hole pair, known as the polaron, has typically been argued.[17,35,42,46,47] However, regarding the electric field effect on the PL intensity of P3HT, single-molecule spectroscopy showed that the electric field was rather inhomogeneous,

[a] *Department of Applied Chemistry, Muroran Institute of Technology, Mizumoto-cho, Muroran 050-8585, Japan*
[b] *Department of Applied Chemistry and Institute of Molecular Science, National Chiao Tung University, 1001, Ta-Hsueh Road, Hsinchu 30010, Taiwan. E-mail: nohta@nctu.edu.tw*
[c] *Center for Emergent Functional Matter Science, National Chiao Tung University, 1001 Ta-Hsueh Rd., Hsinchu 30010, Taiwan*

† Electronic supplementary information (ESI) available: Details of E-A and E-PL spectroscopy and time-resolved E-PL measurements. See DOI: 10.1039/c8cp07801g

and that single molecules showing PL increases and decreases coexisted in a sample.[17] For a derivative of poly(*p*-phenylene), both an increase and decrease in PL intensity were similarly observed in the presence of external electric fields.[36] The mechanism to explain these opposite field effects on the PL intensity is not fully understood. The current-induced quenching of PL has also been observed,[48,49] and so insulation of the P3HT film needs to be investigated to determine the intrinsic electric field effects. Furthermore, PL has been monitored at a fixed wavelength in previous studies, but measurements of electric field effects over the whole PL spectra are essential for elucidating the mechanism of the electric field effects on excitation dynamics. In previous studies, electric field effects were measured by monitoring the field-induced change in PL intensity by applying direct current (DC) fields, but experiments using modulation spectroscopy technique are more suitable for the precise determination of electric field effects on PL.

Herein, we report the measurement of the quadratic response of P3HT PL to electric fields through modulation spectroscopy of the PL spectra, known as electrophotoluminescence (E-PL) spectroscopy. The mechanism of the electric field effects on PL was also studied by measuring field-induced changes in the PL decay profile of P3HT. The quadratic field effect on the absorption spectra of P3HT, namely, electroabsorption (E-A) spectra, were also measured. P3HT was dispersed in an insulating PMMA matrix to prevent the injection of charge carriers into P3HT from electrodes. Based on these results, the electronic structure and dynamics of P3HT following photoexcitation in the absence and presence of external electric field were discussed.

2. Experimental

A fluorine-doped tin-oxide-coated glass (FTO) substrate (Sinonar) was etched using zinc powder and 4 N HCl solution, washed with detergent, water/acetone/isopropanol mixture, and deionized water, and then cleaned using an ultraviolet–ozone cleaner. Poly(methyl methacrylate) (PMMA) (Aldrich, averaged MW = 120 000) was purified by precipitation from a mixture of benzene and methanol, and extraction with hot methanol.

A solution was prepared by dissolving rr-P3HT (0.67 mg; M_n 15 000–45 000, Rieke metals) and PMMA (0.04 g) in benzene (1 mL). The corresponding P3HT concentration was 1 mol% with respect to the amount of PMMA monomer units. We prepared a thin film of P3HT dispersed in PMMA from the P3HT and PMMA solution mixture using a spin-coating technique. A semitransparent silver film was prepared on the P3HT film using a vacuum deposition technique. The silver film and FTO substrate were used as electrodes to apply external electric fields (Fig. 1). The thickness of the P3HT-dispersed PMMA film was measured using a surface roughness meter (Veeco, Dektak 150). In this work, the thickness was approx. 0.6 μm. In PL measurements in solution, P3HT was dissolved in chlorobenzene at a concentration of 1×10^{-6} M.

All measurements were conducted at room temperature. For the E-A measurements, we used an EMV-100 spectrometer

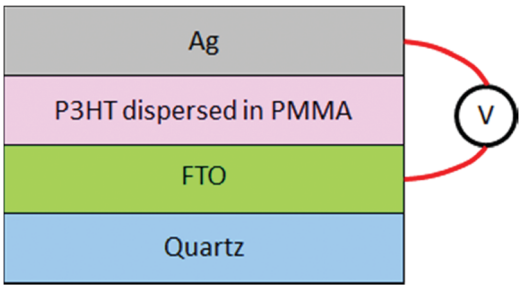

Fig. 1 Layer structure of the device used in the present work. FTO and Ag films were used as electrodes to apply external voltages (V) to P3HT dispersed in a PMMA matrix.

(JASCO), the details of which were reported elsewhere,[50,51] and in the ESI.†

The E-PL spectra, which correspond to the electric-field induced change in PL spectra, were measured using a commercial spectrofluorometer (JASCO, FP777) combined with a lock-in amplifier, the details of which are described elsewhere,[52] and in the ESI.† The PL intensity at zero field and its field-induced change are hereafter represented by I_{PL} and ΔI_{PL} ($\equiv I_{PL}(F \neq 0) - I_{PL}(F = 0)$), respectively. E-PL spectra represent the plots of ΔI_{PL} as a function of wavelength (wavenumber).

PL decay profiles of solid samples in the absence and presence of an electric field were measured using a homemade system. This instrument has been described elsewhere[53] and in the ESI.† Briefly, measurement of the decay profiles was based on a time-correlated single photon counting (TCSPC) technique combined with a femtosecond pulsed laser. A multichannel pulse height analyzer (MCA) was used to obtain PL decay profiles. The field-induced change in decay profiles was obtained using a square-wave voltage pulse train as modulating electric fields. One cycle of the pulse train was composed of the sequence of positive, zero, negative, and zero voltage pulses. In the results, four decay profiles that corresponded to positive, zero, negative, and zero bias could be obtained.

PL decay profiles of P3HT in solution were also measured using a TCSPC system (Fluotime 200, PicoQuant) combined with a picosecond pulsed-diode laser with a pulse width of ~100 ps (LDH-P-C 440, PicoQuant). The repetition rate and pulse energy of the laser used for the experiments in solution were 0.5 MHz and 1 nJ cm^{-2}, respectively.

3. Theoretical background of E-A and E-PL spectroscopy

The field-induced change in absorbance for molecules can be expressed as a linear combination of the zeroth, first, and second derivatives of the absorption spectra:[54–58]

$$\Delta A(\nu) = (fF)^2 \left[A_\chi A(\nu) + B_\chi \nu \frac{d(A(\nu)/\nu)}{d\nu} + C_\chi \nu \frac{d^2(A(\nu)/\nu)}{d^2\nu} \right], \quad (1)$$

where ν is the wavenumber of light, $A(\nu)$ is the absorbance at ν, f is the internal field factor, F (=$|\boldsymbol{F}|$) is the field strength, A_χ,B_χ,

 This journal is © the Owner Societies 2019

and C_χ are the coefficients for the zeroth, first, and second derivatives of $A(\nu)$, respectively, and χ is the angle between the external electric field $\boldsymbol{F}$ and the polarization direction of the excitation light. We now assume that molecules are isotropically oriented, and immobilized in rigid matrices, such as the PMMA film. In experiments with $\chi = 54.7^\circ$, the coefficients B_χ and C_χ in eqn (1) are given by

$$B_\chi = \frac{\Delta\bar{\alpha}}{2hc}, \quad C_\chi = \frac{\Delta\mu^2}{6h^2c^2}. \tag{2}$$

$\Delta\boldsymbol{\alpha}$ is defined as the difference in polarizability tensor ($\Delta\boldsymbol{\alpha} = \boldsymbol{\alpha}_e - \boldsymbol{\alpha}_g$), and $\boldsymbol{\alpha}_e$ and $\boldsymbol{\alpha}_g$ are the polarizabilities of the Franck–Condon excited state and the ground state, respectively. In eqn (2), $\Delta\bar{\alpha}$ is the trace of $\Delta\boldsymbol{\alpha}$, and $\Delta\mu$ (=$|\Delta\boldsymbol{\mu}|$) is the difference between the electric dipole moments of the excited state and ground state,

$$\Delta\bar{\alpha} = \frac{1}{3}\mathrm{Tr}(\boldsymbol{\alpha}_e - \boldsymbol{\alpha}_g), \quad \Delta\boldsymbol{\mu} = \boldsymbol{\mu}_e - \boldsymbol{\mu}_g \tag{3}$$

In eqn (3), $\boldsymbol{\mu}_e$ and $\boldsymbol{\mu}_g$ are the electric dipole moments of the excited state and ground state, respectively. Using these equations, we calculated $\Delta\bar{\alpha}$ and $\Delta\boldsymbol{\mu}$ from the first and second derivative coefficients in the EA spectra, B_χ and C_χ, respectively.

The E-PL spectrum is also given by combining the zeroth, first, and second derivatives of the PL spectrum. For P3HT, as shown later, the coefficient of the zeroth derivative component was of primary importance in the electric field effects on PL, while the contribution of the first and second derivative components to the E-PL spectra was minor. The zeroth derivative component showed the change in PL intensity induced by the external field (ΔI_{PL}) relative to the unperturbed PL intensity (I_{PL}). Electric field effects on photoexcitation dynamics can then be discussed based on the zeroth derivative component of the E-PL spectrum. The mechanism behind the field-induced change in the PL intensity, *i.e.*, in the PL quantum yield, was clarified by studying the field-induced change in fluorescence decay profiles.

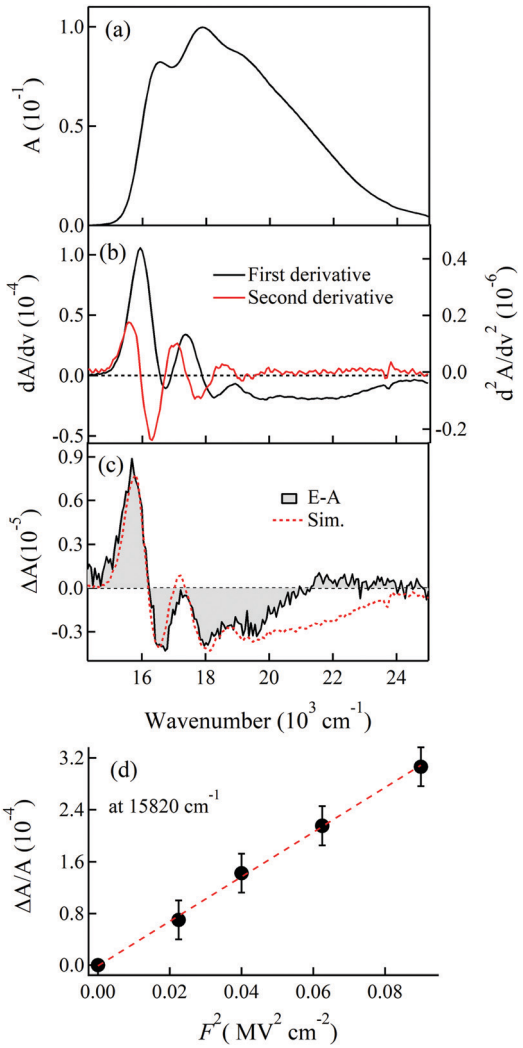

Fig. 2 (a) Absorption spectrum of P3HT dispersed in a PMMA matrix; (b) the first and second derivatives of the absorption spectrum; (c) E-A spectrum observed with a field strength of 0.3 MV cm^{-1}; and (d) plots of the field-induced changes in absorption intensity at 15 820 cm^{-1}. In (c), the black and red lines represent observed and simulated spectra, respectively.

4. Results and discussion

Absorption and E-A spectra

Absorption and E-A spectra of P3HT dispersed in a PMMA matrix are shown in Fig. 2. The magnitude of the field-induced change in absorption intensity was proportional to the square of the applied field strength, as shown in Fig. 2d, as expected from eqn (1). We simulated the E-A spectrum using a sum of the zeroth, first, and second derivative line shapes of the absorption band shown in Fig. 2a and b, as shown in Fig. 2c.

We observed negligibly small contributions from the zeroth-derivative coefficient A_χ (3×10^{-5} MV^{-2} cm^2) to the E-A spectrum, indicating that the transition dipole moment of the absorption band was hardly affected by application of the external electric field $\boldsymbol{F}$. The values of $\Delta\bar{\alpha}$ and $\Delta\mu$ were determined using eqn (2), affording $\Delta\bar{\alpha}$ = 27 Å and $\Delta\mu$ = 1.9 D, with the assumption that the internal field factor f was equal to unity.

Similar E-A experiments for pristine P3HT have been reported by several groups.[15,38,39,44] The principal feature in the E-A spectrum appearing in the range of 15 000 to 19 000 cm^{-1} was assigned to the Stark shift of the low-lying ^1B_u exciton state. Both the absorption spectra and E-A spectra for P3HT in PMMA showed similar features to those of a pristine P3HT film. These results indicated that the structure of P3HT in PMMA was similar to that of a pristine P3HT film. A pristine P3HT film contains both ordered crystalline aggregates and amorphous P3HT chains.[23] Their absorption spectra are different from each other, with the structured bands appearing at lower energies below 19 000 cm^{-1} mainly attributed to crystalline P3HT aggregates.[23] The absorption band of the amorphous region was broad and showed a maximum intensity above 20 000 cm^{-1}. There was a discrepancy between the simulated curve and the observed result in the E-A spectrum in the region above 19 000 cm^{-1}. A similar discrepancy was reported in the previous E-A studies of the pristine P3HT film. This discrepancy might be attributed to the difference in the molecular parameters and absorption spectra between the ordered aggregates and amorphous regions, or to state mixing with the

optically-forbidden $^{m}A_g$ exciton state induced by electric field perturbation.[15,38,39]

PL and E-PL spectra

The photoluminescence (PL) spectrum is shown in Fig. 3a. We were able to decompose the PL spectrum into two bands that showed PL maxima at 1.42×10^4 cm^{-1} (704 nm) and 1.55×10^4 cm^{-1} (645 nm). Hereafter, these bands are denoted as G1 and G2, respectively.

The E-PL spectrum observed at the second harmonic of the modulation frequency is shown in Fig. 3b. As for the E-A spectra, E-PL spectra are usually given by a combination of the zeroth, first, and second derivatives of the PL spectrum. Actually, the shape of the observed E-PL spectra is similar to that of the corresponding PL spectrum with a positive signal, indicating that the PL quantum yield increased in the presence of the electric field. We attempted to simulate the E-PL spectra using a combination of the zeroth, first, and second derivatives of the G1 and G2 bands in the PL spectrum. However, the first and second derivative components were minor in the observed E-PL spectra, and only the zeroth derivative component was important for reproducing the observed E-PL spectra. At an excitation wavelength of 450 nm, ΔA of P3HT was so small that we measured the exact magnitude of the field-induced change in PL spectra. As the zeroth derivative component gave information regarding the field-induced change in emission quantum yield,[52,59] electric field effects on photoexcitation dynamics can be understood from the zeroth derivative component in the E-PL spectrum.

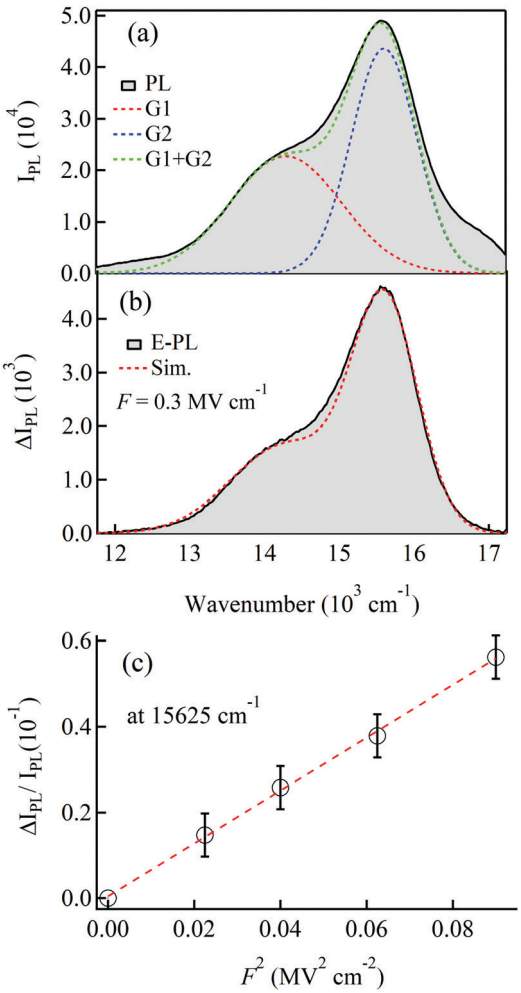

Fig. 3 PL and E-PL spectra with excitation at 450 nm. (a) PL spectrum and decomposition to the G1 and G2 bands, which were used to simulate the E-PL spectrum. (b) E-PL spectrum observed with a field strength of 0.3 MV cm^{-1} (black solid line), and the simulated spectrum (red broken line). (c) Plots of $\Delta I_{PL}/I_{PL}$ as a function of the square of applied field strength. E-PL spectrum was monitored at the second harmonic of the modulation frequency.

The magnitude of $\Delta I_{PL}/I_{PL}$ was proportional to the square of the applied field strength, as shown in Fig. 3c. This result showed that enhancement of the PL quantum yield was due to the quadratic field effect. The magnitudes of the field-induced increase in fluorescence quantum yield were determined to be 7.4% and 9.6% for the G1 and G2 bands, respectively, in the presence of the electric field of 0.3 MV cm^{-1}. The field-induced change in PL intensity can be calculated using $\Delta I_{PL}/I_{PL} = 8.2 \times 10^{-1} \times F^2$ for the G1 band and $\Delta I_{PL}/I_{PL} = 1.1 \times F^2$ for the G2 band, where F is the electric field strength in units of MV cm^{-1}.

The electric field effect on the PL of P3HT dispersed in PMMA was different to that of the pristine P3HT film sandwiched between mesoporous TiO_2 and PMMA films (mp-TiO_2/P3HT/PMMA) or between Sb_2S_3 and PMMA films. For example, the values of $\Delta I_{PL}/I_{PL}$ for mp-TiO_2/P3HT/PMMA were 0.040 and 0.024 for the G1 and G2 bands, respectively, with a field strength of 0.3 MV cm^{-1}.[44] These values were smaller than the aforementioned values for P3HT dispersed in a PMMA matrix, indicating that the field-induced PL quenching was more effective for P3HT dispersed in PMMA than for the P3HT solid film.

Fluorescence quantum yield and its field effect

The absorption and PL spectra of P3HT in solution show very different features to that in a solid film.[12,23] In this work, we reconfirmed the features expected in solution. As shown in Fig. 4, the absorption spectrum of P3HT in chlorobenzene showed a maximum at 2.22×10^4 cm^{-1} (450 nm) with a near-single band. The PL spectrum in solution showed a blue shift compared with that of the film, even when P3HT was distributed in a PMMA matrix (see Fig. 4). Notably, the PL intensity maximum of P3HT was at 1.71×10^4 cm^{-1} ($\sim$586 nm) in solution.

The radiative decay rate constant (k_r) in chlorobenzene solution was calculated using the following equation:[60]

$$k_r = 2.88 \times 10^{-9} n^2 \frac{g_l}{g_u} \frac{\int I_{PL}(\nu) d\nu}{\int \nu^{-3} I_{PL}(\nu) d\nu} \int \varepsilon(\nu) d \ln \nu \qquad (4)$$

where n is the refractive index of the solvent, g_l and g_u are the multiplicities of the ground and excited states, respectively, ν is the wavenumber of light, $I_{PL}(\nu)$ is the intensity of PL at ν, and $\varepsilon(\nu)$ is the molar extinction coefficient at ν. Both g_l and g_u were equal to 1 in the present study, because we were concerned with the fluorescence (PL) of P3HT. The calculated radiative decay rate constant, k_r, of P3HT in chlorobenzene was estimated to be 6.1×10^8 s^{-1}, which was very similar to the value reported by Theander *et al.* for P3HT dissolved in chloroform. (5.6×10^8 s^{-1}).[30]

This journal is © the Owner Societies 2019

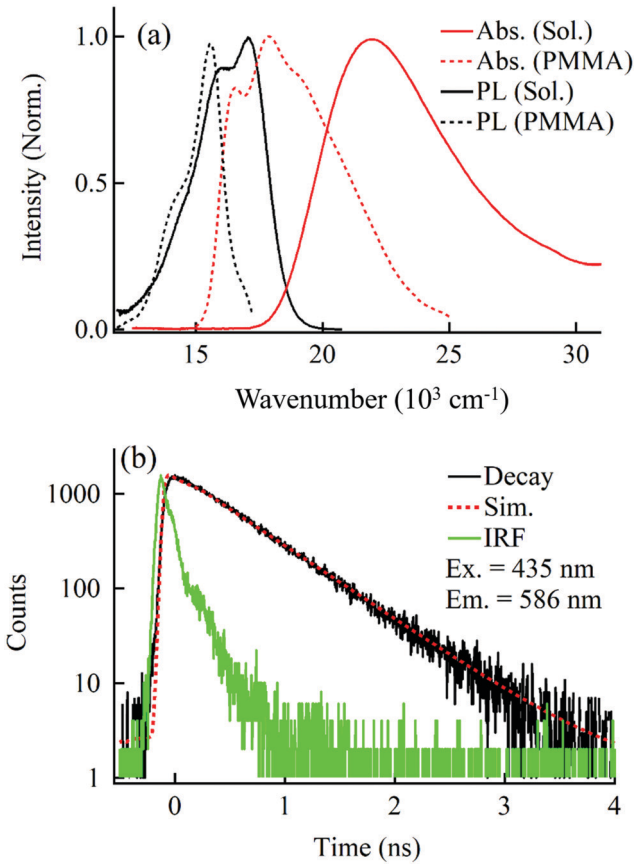

Fig. 4 (a) Absorption spectra (red line) and PL spectra (black line) of P3HT in solution (solid line) and P3HT distributed in a PMMA matrix (broken line). (b) PL decay profile in solution (black line) observed at 586 nm with excitation at 435 nm, the instrumental response function (IRF) (green line), and the decay simulated by assuming a single exponential function (red line). PL spectra in (a) were obtained with excitation at 450 nm.

The fluorescence decay of P3HT in chlorobenzene showed a near-single exponential decay with a lifetime of 560 ps, as shown in Fig. 4, in agreement with the value reported by Cook *et al.*[12] The PL quantum yield (Φ_F) of P3HT in chlorobenzene can be evaluated from the PL lifetime (τ) and k_r using the following equation: $\Phi_F = k_r \times \tau$. The magnitude of Φ_F for P3HT in chlorobenzene was determined to be 0.34, which was also in good agreement with that reported by Cook *et al.* (0.33 ± 0.007).[12]

The value of k_r can also be obtained from the Φ_F and PL lifetime. Using $\Phi_F = 0.33$, which was reported by Cook *et al.* and the PL lifetime of $\tau = 560$ ps observed in this work, we obtained $k_r = 5.9 \times 10^8$ s^{-1}. This result was very close to that estimated from the absorption coefficient using eqn (4).

The PL of P3HT dispersed in a PMMA matrix showed multiexponential decay, even without application of an electric field, as shown in Fig. 5–7. The decay profiles were simulated by assuming a tri-exponential decay function of the form of $\sum_{i=1}^{3} A_i \exp\left(-\frac{t}{\tau_i}\right)$. The preexponential factor and lifetime of each component obtained from the simulation are shown in Table 1. The average lifetime (τ_{ave}), defined by $\sum_{i=1}^{3} A_i\tau_i \Big/ \sum_{i=1}^{3} A_i$, was estimated to be 62 ps for G1 and 64 ps for G2. Using these average lifetimes and assuming that the k_r value for PH3T dispersed in PMMA was the same as that in solution, the magnitude of Φ_F was estimated to be 0.038 for G1 and 0.039 for G2. These values were comparable to the previously reported value of $\Phi = 0.02$ for a pristine P3HT film, which was determined from comparison of the PL spectrum to that of a standard solution of the fluorescence quantum yield.[12]

The similar characteristics of the excited state kinetics and similar features of the absorption and PL spectra between P3HT dispersed in a PMMA matrix and pristine P3HT film should be noted. For P3HT dispersed in PMMA at a low concentration of 1 mol%, we might expect characteristics similar to a solution of P3HT. However, these characteristics were not similar, but were rather similar to those of the P3HT solid film. The PL lifetimes of a pristine P3HT film were measured in our previous work, with similar lifetimes obtained herein. For example, the components with lifetimes of approx. 40 ps and 200 ps observed for a pristine P3HT film were in good agreement with components τ_1 and τ_2 in Table 1. These results suggested that isolated polymer chains did not exist in the PMMA matrix, but that P3HT polymer chains were segregated from the PMMA matrix to form aggregates. Thiessen *et al.* studied the effect of polymer matrices on the P3HT structure using single molecule fluorescence spectroscopy,[26] visualizing the domains of aggregated P3HT in the PMMA matrix using fluorescence micrographs. Furthermore, the PL spectra of P3HT in PMMA resemble those of the P3HT pristine film, while there was a striking difference between the present results and those observed in solution (toluene) and in a Zeonex polymer matrix. These results also suggested the formation of P3HT aggregates in PMMA due to phase separation. Both the P3HT aggregates formed in the PMMA matrix and the P3HT solid film were likely composed of a mixture of crystalline domains with lamellar ordering and an amorphous phase.[11,61,62]

Change in PL decay profile induced by electric fields

From steady-state measurements of the E-PL spectra, we observed an enhancement in the PL quantum yield owing to quadratic electric field effects (Fig. 3). The mechanisms of the electric-field effects on PL intensity can be investigated by measuring the change in PL decay profiles induced by electric fields, because the change in PL quantum yield can be caused by the electric field-induced change in population and/or decay kinetics in the emitting state. The emitting state was not directly produced upon photoexcitation, but after relaxation from the Franck–Condon photoexcited state.[44] If the rate constants of any decay processes from the Franck–Condon photoexcited state were affected by electric fields, the yield of the emitting state should change. Changes in the decay rate constants at the emitting state also lead to changes in the PL quantum yield. Enhancement of the PL quantum yield, as observed in this study, can occur if the sum of the nonradiative decay rate constants of the emitting state are decreased by applying electric fields. The increase in k_r might also result in an increase in the PL quantum yield.

We measured the PL decay profiles in the presence and absence of the electric field of 0.3 MV cm^{-1}. Hereafter, the

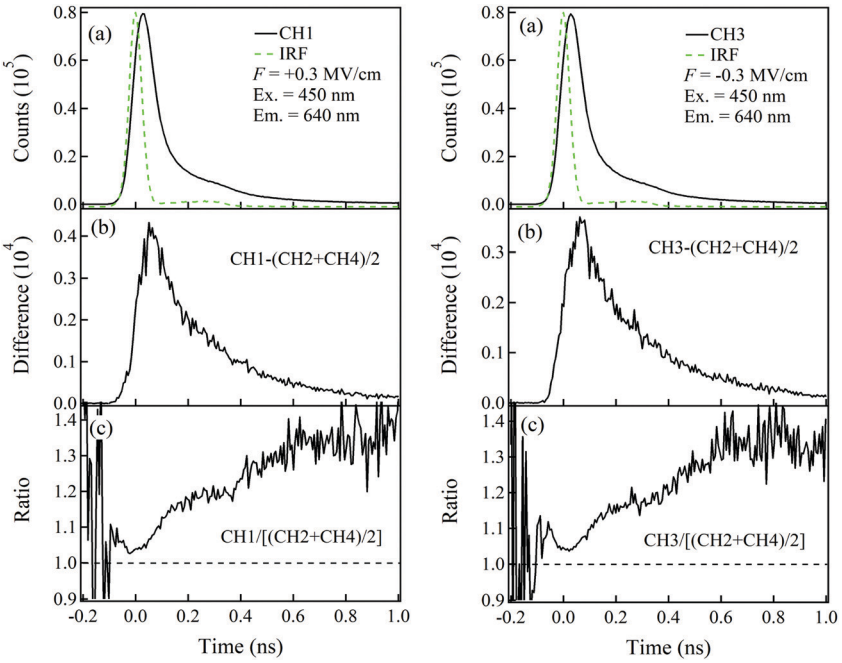

Fig. 5 (a) PL decay profile observed at 640 nm in the presence of +0.3 MV cm^{-1} (CH1, left) and −0.3 MV cm^{-1} (CH3, right); (b) the differences between CH1 and (CH2 + CH4)/2 (left) and between CH3 and (CH2 + CH4)/2 (right); and (c) the ratios of CH1 to (CH2 + CH4)/2 (left) and CH3 to (CH2 + CH4)/2 (right). (CH2 + CH4)/2 corresponds to the decay at zero field.

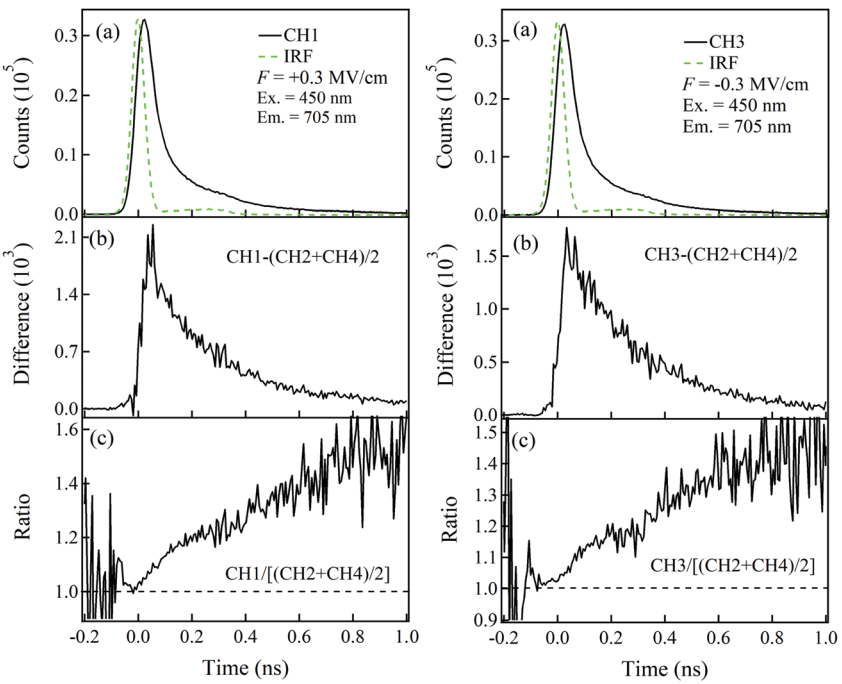

Fig. 6 (a) PL decay profile observed at 705 nm in the presence of +0.3 MV cm^{-1} (CH1, left) and −0.3 MV cm^{-1} (CH3, right); (b) the differences between CH1 and (CH2 + CH4)/2 (left) and between CH3 and (CH2 + CH4)/2 (right); and (c) the ratios of CH1 to (CH2 + CH4)/2 (left) and CH3 to (CH2 + CH4)/2 (right). (CH2 + CH4)/2 corresponds to the decay at zero field.

decay profiles measured in the presence of positive, zero, negative, and zero voltages are denoted as Channels 1 (CH1), 2 (CH2), 3 (CH3), and 4 (CH4), respectively. Measurements of the decay profiles are described in ESI.† In the steady-state E-PL measurements, we measured the quadratic electric field effects on the PL intensity. We investigated changes in the decay profiles that originated from the quadratic electric field effects, as follows. The decay profile in the presence of the electric field

 This journal is © the Owner Societies 2019

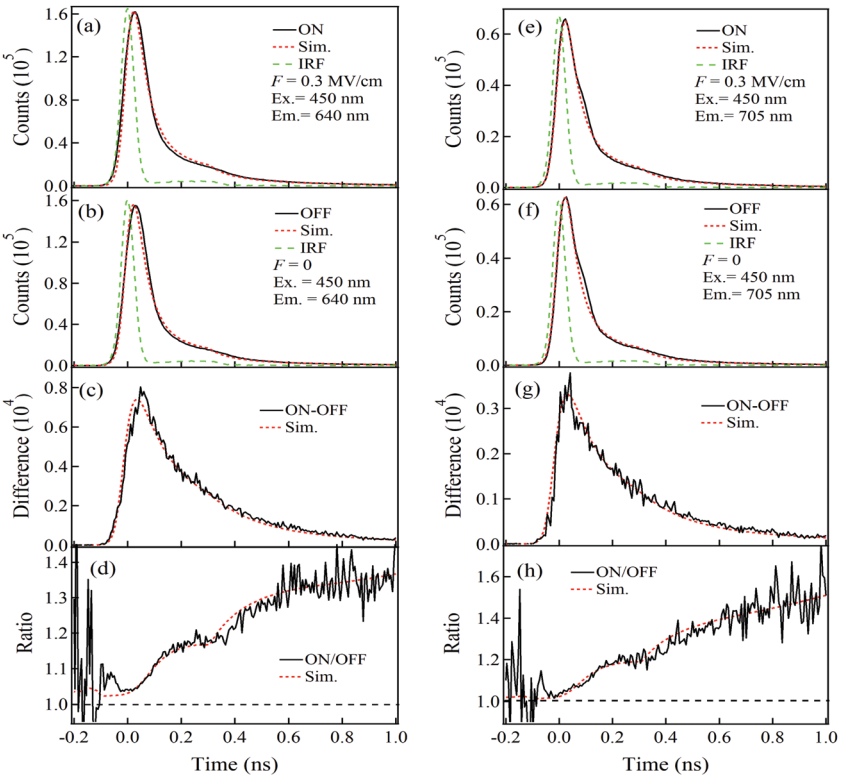

Fig. 7 PL decay profiles in the presence of 0.3 MV cm^{-1} and at zero field monitored at 640 nm (1.56 × 10^4 cm^{-1}) (left column) and at 705 nm (1.41 × 10^4 cm^{-1}) (right column) with excitation at 450 nm. (a and e) Decay profiles of (CH1 + CH3), representing $I(t)_{ON}$; (b and f) decay profile of (CH2 + CH4), representing $I(t)_{OFF}$; (c and g) differences between $I(t)_{ON}$ and $I(t)_{OFF}$; and (d and h) ratios of $I(t)_{ON}$ to $I(t)_{OFF}$. Red lines represent simulations and green lines shown in (a, b, e and f) represent the instrument response function (IRF).

Table 1 Lifetime (τ_i, ps) and pre-exponential factor (given in parentheses) of each decaying component of PL observed at a field strength of 0.3 MV cm^{-1} measured as $I(t)_{ON}$ = CH1 + CH3, and measured as $I(t)_{OFF}$ = CH2 + CH4 at zero field. The average lifetime (τ_{ave}) and the sum of the pre-exponential factors $\left(\sum_{i=1}^{3} A_i\right)$ in each decay profile are also shown. The sum of the pre-exponential factors are normalized to unity for the decay profile at zero field. The PL was monitored at wavelengths λ = 640 and 705 nm for the G2 and G1 bands, respectively

λ (nm)	F (MV cm^{-1})	τ_1 (ps) (A_1)	τ_2 (ps) (A_2)	τ_3 (ps) (A_3)	τ_{ave} (ps) $\left(\sum_{i=1}^{3} A_i\right)$
640	0.3	39.2 (0.754)	130 (0.239)	432 (0.027)	70 ± 4.3 (1.020)
	0	37.8 (0.752)	121 (0.225)	411 (0.023)	64 ± 3.6 (1.000)
705	0.3	37.3 (0.738)	125 (0.246)	438 (0.027)	69 ± 4.2 (1.011)
	0	34.1 (0.732)	111 (0.242)	376 (0.026)	62 ± 3.5 (1.000)

of 0.3 MV cm^{-1} is obtained from the sum of CH1 and CH3, and the decay profile in the absence of the electric field is obtained from the sum of CH2 and CH4. Notably, CH2 and CH4 give essentially the same decay profile, as shown in ESI† (Fig. S2). Hereafter, $I_{ON}(t)$ and $I_{OFF}(t)$ are used to represent the decay profiles obtained from CH1 + CH3 and CH2 + CH4 for F = 0.3 MV cm^{-1} and zero, respectively. CH1 and CH3 show the decay profiles observed in the presence of +0.3 and −0.3 MV cm^{-1}, respectively. The linear electric field effect on PL was expected to drastically affect the field-induced change in the decay profile when the direction of the applied electric field was inverted. This was true for P3HT solid film sandwiched between TiO_2 and PMMA films or sandwiched between Sb_2S_3 and PMMA films.[44] However, in P3HT dispersed in a PMMA matrix, CH1 and CH3 showed very similar electric field effects on the PL decay profile, as shown in Fig. 5 and 6. Therefore, for P3HT polymer chains dispersed in a PMMA matrix, the linear electric field effect on PL was very small or zero, and the quadratic field effect was dominant.

The decay profiles of $I_{ON}(t)$ and $I_{OFF}(t)$ are shown in Fig. 7. The time profile of the difference ($I_{ON}(t) - I_{OFF}(t)$) showed positive signal over the range of the timescale measured in this work (Fig. 7c and g). This result agreed with those of the steady-state E-PL measurements, which indicated an enhancement in the PL intensity in the presence of external electric fields. The intensity of ($I_{ON}(t) - I_{OFF}(t)$) integrated into the whole time range was about 9% of the integrated intensity of $I_{OFF}(t)$, both in G1 and G2, which was in fair agreement with the steady-state experiment. The time profile of the ratio ($I_{ON}(t)/I_{OFF}(t)$) was nearly one at t = 0, indicating that the pre-exponential factors of the each decay component were little affected by the electric field for both G1 and G2. Furthermore, in the time profiles of the ratio, the value increased with time after photoexcitation. This result qualitatively indicated that the decay lifetime was extended in the presence of the electric field.

The above qualitative argument was quantitatively confirmed through analysis of the field-induced change in the PL decay profiles. The lifetimes and pre-exponential factors for $I_{ON}(t)$ and

$I_{OFF}(t)$ were determined by assuming a tri-exponential decay function. The subtle changes in lifetimes and pre-exponential factors induced by the electric fields were precisely determined by simultaneously reproducing the difference and the ratio between $I_{ON}(t)$ and $I_{OFF}(t)$ in the decay analysis. The pre-exponential factors and lifetimes of the three exponential components in the tri-exponential decay function are summarized in Table 1. The average lifetimes, τ_{ave}, increased in the presence of electric fields. The field-induced changes in the pre-exponential factors were minor, showing that the initial population of the emitting state of P3HT was little affected by the electric fields.

As the mechanism of PL quantum yield enhancement observed in the E-PL spectra, we can consider that the sum of nonradiative decay rate constants of the emitting state became smaller in the presence of electric fields. The change in the PL quantum yield ($\Delta\Phi(F)$) induced by $\boldsymbol{F}$ can be related to the change in the sum of the nonradiative decay rate constants ($\Delta k_{nr}(F)$), as follows:[55,59] $\Delta\Phi(F) = -\Delta k_{nr}(F) \times \tau$, where τ is the PL lifetime in the absence of $\boldsymbol{F}$. We can examine this mechanism from the E-PL spectra and decay profile data, taking $\Delta I_{PL}/I_{PL}$ as $\Delta\Phi(F)$, τ_{ave} of $I_{OFF}(t)$ as τ, and the difference between the values of $1/\tau_{ave}$ for $I_{ON}(t)$ and $I_{OFF}(t)$ as $\Delta k_{nr}(F)$. We then obtained $\Delta k_{nr}(F) = -1.3 \times 10^{9}$ s^{-1} at 0.3 MV cm^{-1} and $\tau = 6.4 \times 10^{-11}$ s^{-1} at the PL wavelength of 640 nm for G2. Using these two terms, $\Delta\Phi(F)$ was obtained as 8.3×10^{-2} in the presence of 0.3 MV cm^{-1}. This value was in good agreement with the $\Delta I_{PL}/I_{PL} = 9.6 \times 10^{-2}$ experimentally observed for the G2 band in the E-PL spectrum at 0.3 MV cm^{-1}. Therefore, field-induced enhancement of the PL quantum yield is caused by the change in the sum of the nonradiative rate constants at the PL emitting state. The zeroth derivative component of A_χ in the EA spectrum was negligibly small, in the order of 10^{-5}, and the contribution of the change in the radiative decay rate constant was, therefore, negligible.

Mechanism of field-induced PL enhancement

The PL decay profile results demonstrated that (i) the field-induced enhancement of the PL intensity can be attributed to elongation of the PL lifetime in the presence of electric fields, and (ii) the field-induced change in the population of the emitting state was very small.

It has been suggested that the charge carrier is generated by dissociation of hot (unrelaxed) excitons, with this process taking place promptly.[12,13,44,61,63] This process competes with the generation process of the relaxed singlet exciton. In a pristine P3HT film sandwiched between mp-TiO_2 and PMMA films or between Sb_2S_3 and PMMA films, we hardly observed the change in the preexponential factors induced by quadratic electric field effects, although a change was observed as a result of the first-order electric field effects.[44] In the P3HT film dispersed in PMMA, we obtained similar results for which a change in the preexponential factors was hardly observed. These results indicated that the dissociation rate of the hot exciton produced directly by photoexcitation did not show the quadratic electric field effect because the branching ratio between the emitting state and the charge carriers depends on the dissociation rate of the hot exciton.

The assignment of each decay component observed in the hundreds of femtoseconds to nanosecond timescale range, which has been proposed to date, includes a torsional relaxation toward a planar configuration of thiophene units in P3HT chains with a relaxation time of 13 ps[16] and the exciton diffusion process. This diffusion is explained in terms of downhill relaxation due to energy transfer, in which the excitons migrate toward sites with lower energy levels in the density-of-states (DOS) of the energy band of P3HT.[35,62,64,65] In general, the downhill relaxation of singlet excitons occurs with timescales in the pico- to nanosecond range. The delayed PL, which asymptotically decays with a power law and lasts until $t \geq 10$ ns, has also been observed to originate from the recombination of charge carriers.[17,20,25,66]

We observed that curves of the ratio ($I_{ON}(t)/I_{OFF}(t)$) of the decay profiles became larger as the time windows become larger (Fig. 7d and h). This behavior suggested that the relatively slower dynamics of the exciton and/or charge carriers were significantly affected by electric fields. A value of the ratio greater than 1 corresponds to PL enhancement, with the enhancement factor reaching $\sim$1.4 at 1.0 ns. We proposed that delayed PL due to charge carrier recombination was increased by the quadratic electric-field effects. However, it was noted that the field-induced change in intensity estimated from integration of the PL decay profile was similar to that obtained from the steady-state measurement, as mentioned earlier. This implied that the electric field effect was concerned with the dynamics of P3HT, which occurred on the subnanosecond timescale. We tentatively assigned the lifetime component of τ_3 to the delayed PL. The component τ_3 showed a significant increase resulting from the quadratic electric-field effects (see Table 1). The delayed PL has been reported to show decay obeying a power law in the form of $\approx t^{-(1+\mu)}$, where the parameter μ is given by the ratio of the characteristic electron–hole distance for the distribution of their distances, and the distance dependence (denoted by β) of the tunneling probability of recombination.[20] In this model, the PL decay became slower when the electron–hole distance decreased, or β increased. If any of these changes were induced by electric fields, PL enhancement would consequently be observed. The value of the ratio around $t = 0$ was close to unity, indicating relatively fast dynamics, including conformational planarization, and relaxation of the hot exciton was hardly affected by the electric fields.

We might explain the observed result if the downhill relaxation rate became slower in the presence of electric fields. The field-induced change in the energy transfer rate might be significant if the distribution of the energy levels within the DOS was sparse. The DOS in the P3HT aggregate was unambiguously not sparse, and perturbation of the energy transfer rate might be insignificant. However, we observed a field-induced increase in the PL lifetimes over the timescales in the range of tens to hundreds of picoseconds in the lifetime components of τ_1 and τ_2. These timescales were parallel with those for downhill relaxation, as stated earlier. This might imply that the decrease in the energy transfer rate causing downhill relaxation was induced by electric fields. However, we were unable to clearly interpret the mechanism through which energy transfer of P3HT was reduced by electric field application, and the electric field effect on the delayed fluorescence might be more plausible.

 This journal is © the Owner Societies 2019

Previous studies on electric field effects on the PL of π-conjugated polymers have, in general, shown that the PL is quenched by electric fields. However, we observed the opposite effect, with a field-induced increase in the PL of P3HT dispersed in PMMA. In our previous work on pristine P3HT film, the increase in PL was similarly observed with quadratic electric field effects.[44] Notably, both the increase and quenching of PL were observed in the presence of an electric field when single-molecule spectroscopy was used without ensemble averaging.[17,36] We already investigated the first-order electric field effects for the pristine P3HT film sandwiched between mp-TiO_2 and PMMA films or between Sb_2S_3 and PMMA films, and have reported that both the increase and decrease in the PL intensity were observed depending on the direction of the external electric field.[44] The anisotropy of the field-induced change in PL with respect to the field direction of the applied electric fields can be explained in terms of the synergy effect between the internal electric field, which exists in the P3HT film, and the externally applied electric field.[44] Based on this result, the variation in the electric field effects observed by single-molecule spectroscopy likely resulted from the inhomogeneity in the internal electric fields, which might intrinsically exist due to the local inhomogeneity of the medium and structural fluctuations in the polymer chains. The field-induced quenching of PL reported so far might also be explained by invoking the quenching induced by the current. In the present work, P3HT was dispersed at a dilute concentration in the insulating PMMA film, so we can neglect the contribution of current-induced quenching of the PL. The direction of the electric field can also be a factor that determines the increase or decrease in PL. The previous studies that observed PL quenching employed a static DC electric field in the experiments. The PL quenching observed in previous studies might be induced by the synergy effect between the internal electric field, which might exist for the reasons stated above, and the externally applied electric field. Under this mechanism, we might expect an increase in the PL when the direction of the external DC electric field is reversed. In the present experiments, we used the modulation technique, where the PL signal was detected to be synchronized with the modulation frequency at the second-harmonic of the applied alternating-current (AC) electric field. Furthermore, a linear electric field effect caused by the anisotropic properties of the sample can be neglected in P3HT dispersed in PMMA, in contrast with the P3HT films sandwiched between TiO_2 and PMMA or between Sb_2S_3 and PMMA films. Therefore, we obtained the intrinsic external electric field effects on the PL of P3HT aggregates without the contribution of the internal electric field effects.

5. Conclusions

The dynamics of the excitons in P3HT dispersed in a PMMA film were studied using E-A and E-PL spectroscopy. In a PMMA matrix, the formation of crystalline aggregates is indicated owing to the similarity of the absorption and PL spectra with those of the pristine P3HT film. Previous studies on the electric field effects of π-conjugated polymers including P3HT on the PL have generally reported PL quenching. In contrast, an increase in the PL intensity was observed in this study owing to quadratic electric field effects. The field-induced increase in PL intensity was more effective in P3HT dispersed in a PMMA matrix compared with the pristine P3HT film. Measurement of the field-induced change in PL decay profiles showed that the increase in PL intensity was due to the decrease in the nonradiative decay rate constant, which was mainly attributed to the increase in delayed PL due to charge carrier recombination in the presence of electric fields.

Conflicts of interest

The authors declare no competing financial interests.

Acknowledgements

The Ministry of Science and Technology (MOST) in Taiwan provided financial support for this research (MOST107-2113-M-009-005, MOST107-3017-F009-003). This work was also financially supported by the Center for Emergent Functional Matter Science of National Chiao Tung University from The Featured Areas Research Center Program within the framework of the Higher Education Sprout Project by the Ministry of Education (MOE) in Taiwan.

References

1 W. Barford, *Electronic and optical properties of conjugated polymers*, Oxford University Press, Oxford, 2005.
2 P. Bujak, I. Kulszewicz-Bajer, M. Zagorska, V. Maurel, I. Wielgus and A. Pron, *Chem. Soc. Rev.*, 2013, **42**, 8895–8999.
3 S. Günes, H. Neugebauer and N. S. Sariciftci, *Chem. Rev.*, 2007, **107**, 1324–1338.
4 T. M. Clarke and J. R. Durrant, *Chem. Rev.*, 2010, **110**, 6736–6767.
5 F. C. Spano and C. Silva, *Annu. Rev. Phys. Chem.*, 2014, **65**, 477–500.
6 O. Ostroverkhova, *Chem. Rev.*, 2016, **116**, 13279–13412.
7 O. Itaru and T. Kazuo, *Adv. Mater.*, 2017, **29**, 1605218.
8 A. Facchetti, *Chem. Mater.*, 2011, **23**, 733–758.
9 L. Ying, F. Huang and G. C. Bazan, *Nat. Commun.*, 2017, **8**, 14047.
10 H. Sirringhaus, P. J. Brown, R. H. Friend, M. M. Nielsen, K. Bechgaard, B. M. W. Langeveld-Voss, A. J. H. Spiering, R. A. J. Janssen, E. W. Meijer, P. Herwig and D. M. de Leeuw, *Nature*, 1999, **401**, 685–688.
11 H. Sirringhaus, *Adv. Mater.*, 2005, **17**, 2411–2425.
12 S. Cook, A. Furube and R. Katoh, *Energy Environ. Sci.*, 2008, **1**, 294–299.
13 J. Guo, H. Ohkita, H. Benten and S. Ito, *J. Am. Chem. Soc.*, 2009, **131**, 16869–16880.
14 X. M. Jiang, R. Österbacka, O. Korovyanko, C. P. An, B. Horovitz, R. A. J. Janssen and Z. V. Vardeny, *Adv. Funct. Mater.*, 2002, **12**, 587–597.

15 R. Österbacka, C. P. An, X. M. Jiang and Z. V. Vardeny, *Science*, 2000, **287**, 839–842.
16 P. Parkinson, C. Müller, N. Stingelin, M. B. Johnston and L. M. Herz, *J. Phys. Chem. Lett.*, 2010, **1**, 2788–2792.
17 T. Sugimoto, S. Habuchi, K. Ogino and M. Vacha, *J. Phys. Chem. B*, 2009, **113**, 12220–12226.
18 A. K. Thomas, H. A. Brown, B. D. Datko, J. A. Garcia-Galvez and J. K. Grey, *J. Phys. Chem. C*, 2016, **120**, 23230–23238.
19 N. Banerji, S. Cowan, E. Vauthey and A. J. Heeger, *J. Phys. Chem. C*, 2011, **115**, 9726–9739.
20 F. Paquin, G. Latini, M. Sakowicz, P.-L. Karsenti, L. Wang, D. Beljonne, N. Stingelin and C. Silva, *Phys. Rev. Lett.*, 2011, **106**, 197401.
21 P. J. Brown, D. S. Thomas, A. Köhler, J. S. Wilson, J.-S. Kim, C. M. Ramsdale, H. Sirringhaus and R. H. Friend, *Phys. Rev. B: Condens. Matter Mater. Phys.*, 2003, **67**, 064203.
22 P. J. Brown, H. Sirringhaus, M. Harrison, M. Shkunov and R. H. Friend, *Phys. Rev. B: Condens. Matter Mater. Phys.*, 2001, **63**, 125204.
23 J. Clark, C. Silva, R. H. Friend and F. C. Spano, *Phys. Rev. Lett.*, 2007, **98**, 206406.
24 K. E. Ziemelis, A. T. Hussain, D. D. C. Bradley, R. H. Friend, J. Rühe and G. Wegner, *Phys. Rev. Lett.*, 1991, **66**, 2231–2234.
25 F. Paquin, J. Rivnay, A. Salleo, N. Stingelin and C. Silva-Acuna, *J. Mater. Chem. C*, 2015, **3**, 10715–10722.
26 A. Thiessen, J. Vogelsang, T. Adachi, F. Steiner, D. Vanden Bout and J. M. Lupton, *Proc. Natl. Acad. Sci. U. S. A.*, 2013, **110**, E3550–E3556.
27 B. Ferreira, P. F. da Silva, J. S. Seixas de Melo, J. Pina and A. Maçanita, *J. Phys. Chem. B*, 2012, **116**, 2347–2355.
28 C. Deibel, D. Mack, J. Gorenflot, A. Schöll, S. Krause, F. Reinert, D. Rauh and V. Dyakonov, *Phys. Rev. B: Condens. Matter Mater. Phys.*, 2010, **81**, 085202.
29 O. J. Korovyanko, R. Österbacka, X. M. Jiang, Z. V. Vardeny and R. A. J. Janssen, *Phys. Rev. B: Condens. Matter Mater. Phys.*, 2001, **64**, 235122.
30 M. Theander, O. Inganäs, W. Mammo, T. Olinga, M. Svensson and M. R. Andersson, *J. Phys. Chem. B*, 1999, **103**, 7771–7780.
31 J. Cabanillas-Gonzalez, G. Grancini and G. Lanzani, *Adv. Mater.*, 2011, **23**, 5468–5485.
32 M. S. Mehata, C.-S. Hsu, Y.-P. Lee and N. Ohta, *J. Phys. Chem. B*, 2010, **114**, 6258–6265.
33 P. R. Hania, D. Thomsson and I. G. Scheblykin, *J. Phys. Chem. B*, 2006, **110**, 25895–25900.
34 I. Scheblykin, G. Zoriniants, J. Hofkens, S. De Feyter, M. Van der Auweraer and F. C. De Schryver, *ChemPhysChem*, 2003, **4**, 260–267.
35 I. G. Scheblykin, A. Yartsev, T. Pullerits, V. Gulbinas and V. Sundstrom, *J. Phys. Chem. B*, 2007, **111**, 6303.
36 F. Schindler, J. M. Lupton, J. Müller, J. Feldmann and U. Scherf, *Nat. Mater.*, 2006, **5**, 141.
37 T. M. Smith, J. Kim, L. A. Peteanu and J. Wildeman, *J. Phys. Chem. C*, 2007, **111**, 10119–10129.
38 M. Liess, S. Jeglinski, Z. V. Vardeny, M. Ozaki, K. Yoshino, Y. Ding and T. Barton, *Phys. Rev. B: Condens. Matter Mater. Phys.*, 1997, **56**, 15712–15724.
39 K. Sakurai, H. Tachibana, N. Shiga, C. Terakura, M. Matsumoto and Y. Tokura, *Phys. Rev. B: Condens. Matter Mater. Phys.*, 1997, **56**, 9552–9556.
40 J. D. McNeill, D. B. O'Connor, D. M. Adams, P. F. Barbara and S. B. Kämmer, *J. Phys. Chem. B*, 2001, **105**, 76–82.
41 R. Kersting, U. Lemmer, R. F. Mahrt, K. Leo, H. Kurz, H. Bässler and E. O. Göbel, *Phys. Rev. Lett.*, 1993, **70**, 3820–3823.
42 R. Kersting, U. Lemmer, M. Deussen, H. J. Bakker, R. F. Mahrt, H. Kurz, V. I. Arkhipov, H. Bässler and E. O. Göbel, *Phys. Rev. Lett.*, 1994, **73**, 1440–1443.
43 V. I. Arkhipov, H. Bässler, M. Deussen, E. O. Göbel, R. Kersting, H. Kurz, U. Lemmer and R. F. Mahrt, *Phys. Rev. B: Condens. Matter Mater. Phys.*, 1995, **52**, 4932–4940.
44 T. Iimori, K. Awasthi, C.-S. Chiou, E. W.-G. Diau and N. Ohta, *ACS Appl. Energy Mater.*, 2018, **1**, 6136–6151.
45 M. Deussen, M. Scheidler and H. Bässler, *Synth. Met.*, 1995, **73**, 123–129.
46 W. Graupner, G. Cerullo, G. Lanzani, M. Nisoli, E. J. W. List, G. Leising and S. De Silvestri, *Phys. Rev. Lett.*, 1998, **81**, 3259–3262.
47 V. Gulbinas, Y. Zaushitsyn, V. Sundström, D. Hertel, H. Bässler and A. Yartsev, *Phys. Rev. Lett.*, 2002, **89**, 107401.
48 E. T. Niles, J. D. Roehling, H. Yamagata, A. J. Wise, F. C. Spano, A. J. Moulé and J. K. Grey, *J. Phys. Chem. Lett.*, 2012, **3**, 259–263.
49 A. J. Ferguson, N. Kopidakis, S. E. Shaheen and G. Rumbles, *J. Phys. Chem. C*, 2008, **112**, 9865–9871.
50 H.-C. Chiang, T. Iimori, T. Onodera, H. Oikawa and N. Ohta, *J. Phys. Chem. C*, 2012, **116**, 8230–8235.
51 J. Tayama, T. Iimori and N. Ohta, *J. Chem. Phys.*, 2009, **131**, 244509.
52 N. Ohta, *Bull. Chem. Soc. Jpn.*, 2002, **75**, 1637–1655.
53 M. Tsushima, T. Ushizaka and N. Ohta, *Rev. Sci. Instrum.*, 2004, **75**, 479–485.
54 S. G. Boxer, *J. Phys. Chem. B*, 2009, **113**, 2972–2983.
55 N. Ohta, *Pure Appl. Chem.*, 2013, **85**, 1427–1435.
56 W. Liptay, in *Excited States*, ed. E. C. Lim, Academic Press, New York, 1974, vol. 1, p. 129.
57 S. A. Locknar, A. Chowdhury and L. A. Peteanu, *J. Phys. Chem. B*, 2000, **104**, 5816–5824.
58 E. Jalviste and N. Ohta, *J. Photochem. Photobiol., C*, 2007, **8**, 30–46.
59 T. Iimori, R. Ito and N. Ohta, *J. Phys. Chem. A*, 2016, **120**, 5497–5503.
60 S. J. Strickler and R. A. Berg, *J. Chem. Phys.*, 1962, **37**, 814–822.
61 J. Piris, T. E. Dykstra, A. A. Bakulin, P. H. M. v. Loosdrecht, W. Knulst, M. T. Trinh, J. M. Schins and L. D. A. Siebbeles, *J. Phys. Chem. C*, 2009, **113**, 14500–14506.
62 Y. Tamai, H. Ohkita, H. Benten and S. Ito, *J. Phys. Chem. Lett.*, 2015, **6**, 3417–3428.
63 C. X. Sheng, M. Tong, S. Singh and Z. V. Vardeny, *Phys. Rev. B: Condens. Matter Mater. Phys.*, 2007, **75**, 085206.
64 F. Laquai, Y.-S. Park, J.-J. Kim and T. Basché, *Macromol. Rapid Commun.*, 2009, **30**, 1203–1231.
65 I. Hwang and G. D. Scholes, *Chem. Mater.*, 2011, **23**, 610–620.
66 J. A. Labastide, M. Baghgar, I. Dujovne, B. H. Venkatraman, D. C. Ramsdell, D. Venkataraman and M. D. Barnes, *J. Phys. Chem. Lett.*, 2011, **2**, 2089–2093.

 This journal is © the Owner Societies 2019